



Universiteit
Leiden
The Netherlands

Biomimetic models of [NiFe] hydrogenase for electrocatalytic hydrogen evolution

Gezer, G.

Citation

Gezer, G. (2017, October 10). *Biomimetic models of [NiFe] hydrogenase for electrocatalytic hydrogen evolution*. Retrieved from <https://hdl.handle.net/1887/58770>

Version: Not Applicable (or Unknown)

License: [Licence agreement concerning inclusion of doctoral thesis in the Institutional Repository of the University of Leiden](#)

Downloaded from: <https://hdl.handle.net/1887/58770>

Note: To cite this publication please use the final published version (if applicable).

Cover Page



Universiteit Leiden



The handle <http://hdl.handle.net/1887/58770> holds various files of this Leiden University dissertation

Author: Gezer, G.

Title: Biomimetic models of [NiFe] hydrogenase for electrocatalytic hydrogen evolution

Issue Date: 2017-10-10

Chapter 4

Dealkylation through C–S and Ni–S bond cleavage relevant to the mechanism of methyl-coenzyme M reductase (MCR)

Abstract

With the tridentate ligands H_2ebSmS (3,6-dithia-2,2,7,7-tetramethyloctane-1,8-dithiol), $H_2ebSmSe$ (3,6-dithia-2,2,7,7-tetramethyloctane-1,8-diselenol) and $H_2pbSmSe$ (3,7-dithia-2,2,8,8-tetramethylnonane-1,9-diselenol) two nickel complexes were obtained. The compound $[Ni(pbSmSe)]$ has the expected square-planar geometry, but in $[Ni_2(ebSmS)_2]$ the restricted coordination angle of the ethylene bridge results in an unusual dinuclear compound in which the nickel ions are in square-pyramidal geometries. The intended four-coordinate, square-planar nickel compounds of these ligands appear to be reactive and readily decompose with loss of one of the alkylthiolate or alkylselenolate arms, resulting in dinuclear complexes of new tridentate ligands. Thus, the novel dinuclear 5-coordinate nickel(II) dithioether-dithiolato complex $[Ni_2(ebSmS)_2]$, possessing an unusual coplanar structure and $Ni\cdots H$ anagostic interactions, decomposes in the presence of light through C–S and Ni–S bond cleavage to yield another dinuclear nickel(II) complex of a new asymmetric tridentate thioether-dithiolate ligand. Similar behaviour is observed for the mononuclear nickel(II) dithioether-diselenolato complex $[Ni(pbSmSe)]$, which in the presence of light yields a dinuclear nickel(II) complex of a new asymmetric tridentate thioether-thiolate-selenolate ligand. The compound $[Ni(ebSmSe)]$ is the most reactive as it could not be isolated; instead only the ‘decomposed’ compound was obtained.

This chapter is to be submitted for publication: G. Gezer, R. Angamuthu, W. Roorda, M. A. Siegler, M. Lutz, A. L. Spek and E. Bouwman.

‘Parts of this chapter have been reported in R. Angamuthu PhD Thesis, *Structural and Functional Models for [NiFe] Hydrogenase*, Leiden University, Leiden, 2009.’

4.1 Introduction

Metal thiolates, especially nickel thiolates, are enjoying much attention among bioinorganic and organometallic chemists; they are important in the context of structural and/or functional models for enzymes such as hydrogenases (H_2 ase),¹ superoxide dismutases (SOD),^{2,3} carbon monoxide dehydrogenase/acetylcoenzyme A synthase (CODH/ACS)^{4,5} and methyl coenzyme M reductase (MCR).^{6,7,8} Moreover, the research efforts of the biomimetic community have been directed to the selenium-containing proteins; recently a number of biomimetic compounds as models for the active site in the enzymes containing a selenocysteine in their active site have been reported, in which thiolate donor atoms have been substituted by selenolates.^{9,10} MCR is a key enzyme in biological methane formation by methanogenic archaea. Coenzyme F430 in MCR, a Ni-tetrahydrocorphinoid (Figure 4.1), catalyzes the reaction of methyl-coenzyme M (CH_3 -SCoM; methylthioethyl sulfonate) with coenzyme B (HS-CoB; 7-mercaptoheptanoyl-threonine phosphate) to form methane and the disulfide Co-S-S-CoB.^{6,7} In the past years two widely accepted mechanistic pathways have been proposed for this reaction from the results of a number of experimental and theoretical studies on F430.⁶ The key question to be resolved was whether the catalysis involves a nucleophilic attack of the Ni(I) centre of F430 on the methyl group of CH_3 -SCoM (in the presence of H^+) to form a Ni(III)- CH_3 intermediate (and HS-CoM), or that the Ni(I) centre attacks the thioether sulfur of CH_3 -SCoM to form a Ni(II)-SCoM intermediate (and a CH_3^\bullet radical).^{7,11-13} Recently, new investigations have been done in order to understand reaction mechanism of methyl-coenzyme M and Ni(II)-thiolate was identified as an intermediate.¹⁴

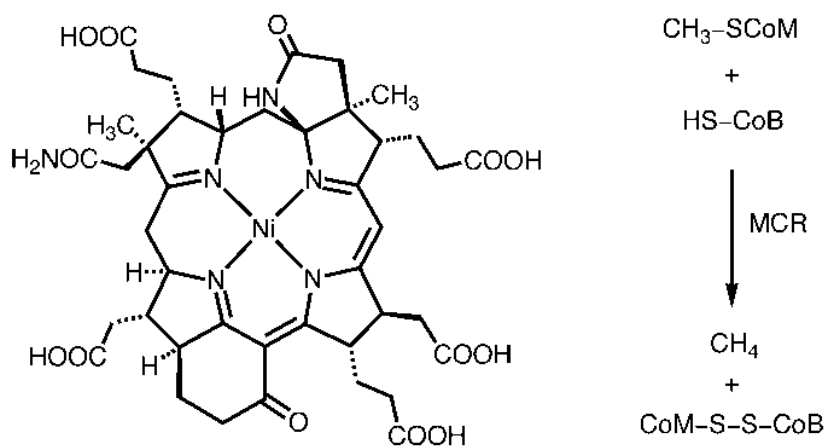


Figure 4.1: Structure of coenzyme F430 (left) and the reaction catalysed by MCR (right).

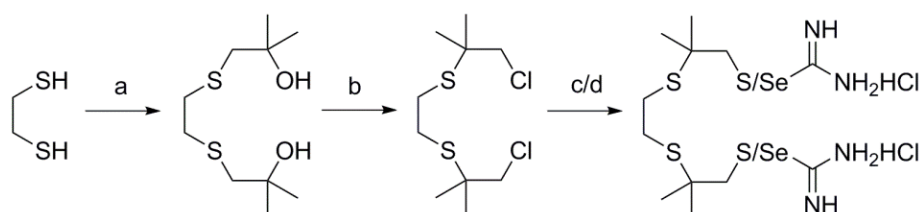
On the other hand, *S*-dealkylation is an industrially important process as it plays a role in desulfurization techniques or in alkyl transfer reactions toward new organosulfur compounds. In contrast to the ubiquitous *S*-dealkylation of terminal alkyl groups of organosulfur ligands involving C–S bond cleavage,¹⁵⁻¹⁸ dealkylation involving both C–S and Ni–S bond cleavage is rather less common, and is reported only to occur in strongly reducing conditions.¹⁹⁻²⁰ The focus of our research includes the study of the synthesis and reactivity of nickel thiolate and selenolate compounds in relation with the structures and functions of nickel-containing enzymes. Reported herein are the synthesis of the thiouronium precursor to a new chelating tetradentate S₄-donor dithioether-dithiolate ligand and the corresponding selenouronium precursor of the tetradentate S₂Se₂-donor dithioether-diselenolate ligand and their nickel complexes. It is shown that upon irradiation of the nickel complexes new dinuclear nickel compounds are formed of asymmetric tridentate dianionic ligands.

4.2 Results

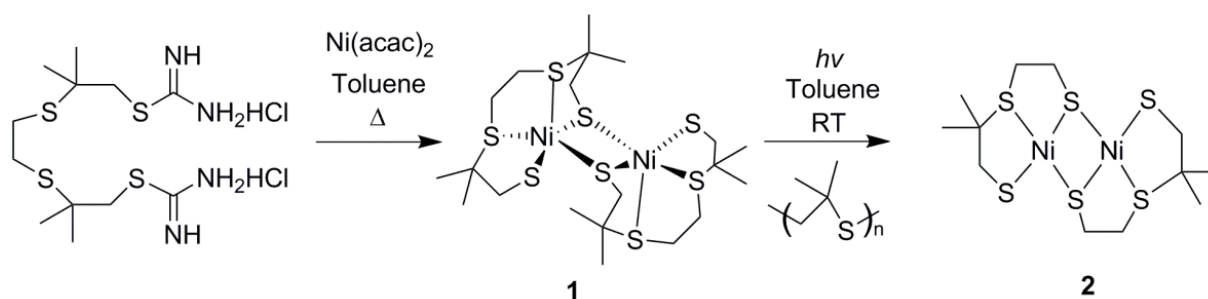
4.2.1 Synthesis and Characterization

The thiouronium and selenouronium salts of the ligands, convenient and easy to handle precursors for the dithiolate and diselenolate ligands H₂ebSmS and H₂ebSmSe, were synthesized in three reaction steps starting from 1,2-ethanedithiol, and were obtained as white powders in high purities and in 76% and 85% yield, respectively (Scheme 4.1). The reaction of Ni(acac)₂ (Hacac = acetylacetonate) with one equivalent of the dithiouronium dichloride precursor of the ligand H₂ebSmS in toluene, in the presence of two equivalents of tetramethylammonium hydroxide resulted in an immediate color change of the initial pale green solution to deep brown (Scheme 4.2). The new nickel complex [Ni₂(ebSmS)₂] (**1**) was isolated as a reddish-brown powder in 63% yield and characterized by single crystal X-ray crystallography, mass spectrometry and elemental analysis. The compound (**1**) gives broad signals in ¹H NMR spectra. Single crystals of (**1**) suitable for X-ray structure determination were obtained within hours from a dichloromethane solution. Unexpectedly, allowing a solution of (**1**) in acetonitrile to stand for 2 weeks resulted in crystals of the dinuclear compound [Ni₂(emSmS)₂] (**2**) (H₂emSmS = 2,2-dimethyl-3-thiapentane-1,5-dithiol), as evidenced by X-ray structure determination. The nickel complex (**3**) was isolated as a dark green powder from the reaction of Ni(acac)₂ with one equivalent of the diselenouronium dichloride precursor of the ligand H₂pbSmSe in ethanol in the presence of two equivalents of tetramethylammonium hydroxide; the characterization and crystal structure of (**3**) has been

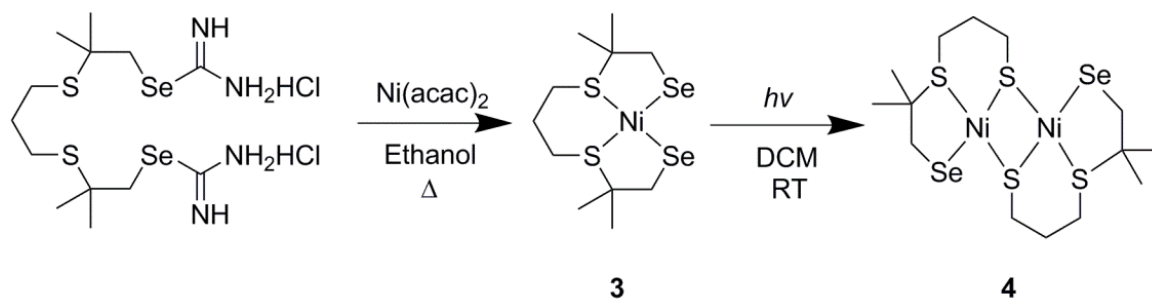
reported.²¹ Single crystals of **(3)** were obtained by vapor diffusion of pentane into dichloromethane solutions of the complexes in dark. Again, unexpectedly crystals of the ‘decomposed’ compound $[\text{Ni}_2(\text{pmSmSe})_2]$ **(4)** ($\text{H}_2\text{pmSmSe} = 2,2\text{-dimethyl-3-thiahexane-1-selenol-6-thiol}$) were obtained by vapor diffusion of pentane into dichloromethane solution of **(3)** in 2-3 weeks as evidenced by X-ray structure determination. The reaction of $\text{Ni}(\text{acac})_2$ with one equivalent of the diselenouronium dichloride precursor of the ligand H_2ebSmSe in ethanol in the presence of two equivalents of tetramethylammonium hydroxide did not result in the formation of the expected compound $[\text{Ni}(\text{ebSmSe})]$ **(5)** or its dinuclear analog similar to **(1)**. Instead the nickel complex $[\text{Ni}_2(\text{ebSmSe})_2]$ **(6)** ($\text{H}_2\text{emSmSe} = 2,2\text{-dimethyl-3-thiapentane-1-selenol-5-thiol}$) was isolated as a brown powder in 52% yield, as shown by single crystal X-ray crystallography, mass spectrometry and elemental analysis. Single crystals of **(6)** were obtained by vapor diffusion of pentane into a dichloromethane solution of the complex.



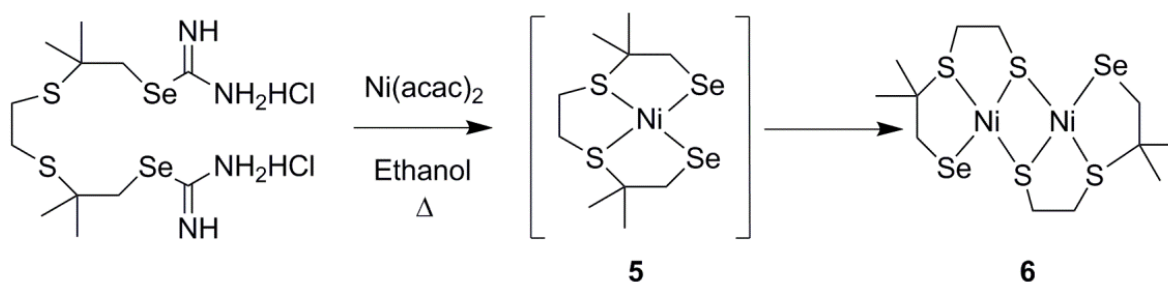
Scheme 4.1: Synthesis of the thiouronium and selenouronium salt precursors for the ligands H_2ebSmS and H_2ebSmSe . (a) $\text{ClCH}_2\text{C}(\text{CH}_3)_2\text{OH}$, NaOH , ethanol, Δ , (b) SOCl_2 , CHCl_3 , RT, (c) $\text{S}=\text{C}(\text{NH}_2)_2$, ethanol, Δ , (d) $\text{Se}=\text{C}(\text{NH}_2)_2$ ethanol, Δ .



Scheme 4.2: Schematic drawing of $[\text{Ni}_2(\text{ebSmS})_2]$ **(1)** and the formation of $[\text{Ni}_2(\text{emSmS})_2]$ **(2)** and oligo-isobutylene sulfide upon irradiation.



Scheme 4.3: Schematic drawing of $[\text{Ni}(\text{pbSmSe})]$ (**3**) and the formation of $[\text{Ni}_2(\text{pmSmSe})_2]$ (**4**) upon irradiation.



Scheme 4.4: Schematic drawing of synthesis of $[\text{Ni}_2(\text{emSmSe})_2]$ (**6**), assumedly via the reactive intermediate $[\text{Ni}(\text{ebSmSe})]$ (**5**).

4.2.2 Description of the Structures

A projection of the molecular structure of the complex (**1**) is shown in Figure 4.2a; selected bond distances and angles are listed in Table 4.1. The asymmetric unit of (**1**) contains one molecule of the dinuclear complex and one molecule of dichloromethane. Two thiolate sulfur donors from the same ligand coordinate to a nickel centre in *trans* positions of each NiS_4 basal plane. One of these thiolate sulfur atoms is bound in a terminal position, whereas the other thiolate is bridging to the adjacent nickel centre. One of the thioether sulfur donors of one ligand and the bridging thiolate sulfur from the other ligand occupy the remaining two *trans* positions in the basal plane; the remaining thioether of the ligand binds in the apical position of the Ni(II) centre. One of the ligands in (**1**) is disordered over two conformations: the major component is related by an approximate two fold axis to the other ligand, the minor component is related by an approximate inversion centre. As a result, one rather short Ni–S thioether distance (Ni1A–S19B, 2.139(4) Å) is observed in the minor component. The τ value, used to describe five-coordinate compounds, for complex (**1**) was calculated to be 0.13 and 0.15 for the two Ni centers, indicating that the geometry of the nickel ion is slightly distorted square pyramidal.

Projections of the molecular structures of the complexes **(2)**, **(4)** and **(6)** are shown in Figure 4.2b and 4.3; selected bond distances and angles are listed in Table 4.1 and 4.2. The compounds **(2)**, **(4)** and **(6)** are highly similar dinuclear nickel complexes comprising different asymmetric tridentate ligands that are derived from the parent tetradentate ligands by loss of one isobutylene-thiol/selenol arm. The asymmetric unit of **(2)** contains one dinuclear nickel complex of the tridentate thioether-dithiolate ligand (emSmS^{2-}) and the asymmetric units of **(4)** and **(6)** contain the dinuclear nickel(II) compounds with the tridentate thioether-thiolate-selenolate ligands (pmSmSe^{2-} and emSmSe^{2-}). The compounds **(2)** and **(6)** have quite similar butterfly cores with hinge angles of 77.70° and 76.76° , respectively. However changing the ethylene bridge to propylene in compound **(4)** results in a smaller hinge angle of 64.99° . The $\text{Ni-S}_{\text{thiolate}}$ and $\text{Ni-Se}_{\text{selenolate}}$ distances are slightly longer than the $\text{Ni-S}_{\text{thioether}}$ distances for complex **(2)**, **(4)** and **(6)**. This observation is in contrast to previous reports,^{4,22-25} but is not unprecedented especially for complex **(4)** and **(6)** due to the larger ionic radius of selenium.²⁶⁻²⁸ In contrast to the common butterfly or folded structures as in **(2)**, **(4)**, **(6)** and other dinuclear or oligonuclear nickel thiolate complexes,^{25,29} the molecular structure of complex **(1)** exhibits an unusual coplanar structure of the two basal planes of the nickel coordination geometries. The dihedral angle between the two basal NiS_4 planes in complex **(1)** is only $2.99(7)^\circ$. This structure may be due to the $\text{Ni}\cdots\text{H}_{\text{Me}}$ anagostic interactions (2.66 \AA and 2.74 \AA) with $\text{Ni}\cdots\text{H-C}$ angles of 132.76° and 132.87° , which may be strong enough to not allow the NiS_4 planes to fold (Fig. 4.2a).³⁰ In literature the anagostic interaction is described by $\text{M}\cdots\text{H-C}$ distances of $\sim 2.3\text{-}2.9 \text{ \AA}$ and $\text{M}\cdots\text{H-C}$ angles of $\sim 110\text{-}170^\circ$.³¹ Complex **(1)** has the shortest $\text{Ni}\cdots\text{H}_{\text{Me}}$ distances compared to other structures (Table 4.3).

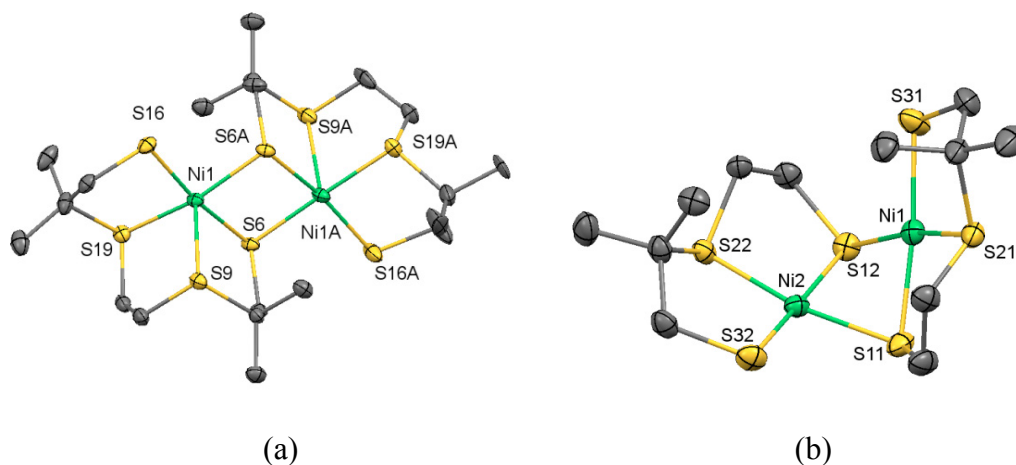


Figure 4.2: Displacement ellipsoid plot (50% probability level) of $[\text{Ni}_2(\text{ebSmS})_2]$ (**1**) (a) at 110(2) K and $[\text{Ni}_2(\text{emSmS})_2]$ (**2**) (b) at 150(2) K. Lattice dichloromethane molecules, partial disorder and hydrogen atoms are omitted for clarity.

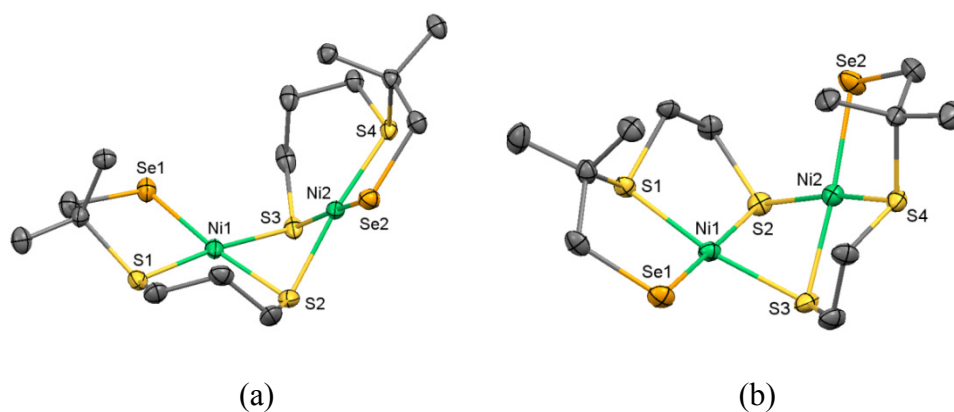


Figure 4.3: Displacement ellipsoid plots (50% probability level) of $[\text{Ni}_2(\text{pmSmSe})_2]$ (**4**) (a) and $[\text{Ni}_2(\text{emSmSe})_2]$ (**6**) (b) at 100(2) K. Hydrogen atoms are omitted for clarity.

Table 4.1: Selected bond lengths (Å) and angles (°) for the complexes **(1)** and **(2)**.

Distances (Å)	(1)	Distances(Å)	(2)
Ni1-S6	2.2345(11)	Ni1-S31	2.1604(6)
Ni1-S9	2.6010(11)	Ni2-S32	2.1559(5)
Ni1-S16	2.1928(11)	Ni1-S21	2.1387(5)
Ni1-S19	2.2359(12)	Ni2-S12	2.2057(5)
Ni1-S6A	2.2096(12)	Ni1-S11	2.2107(6)
Ni1A-S6	2.2139(12)	Ni2-S22	2.1347(5)
Ni1A-S6A	2.2285(12)	Ni1-S12	2.1783(5)
Ni1A-S9A	2.7038(12)	Ni2-S11	2.1818(6)
Ni1A-S16A	2.1966(13)		
Ni1A-S19A	2.246(3)		
Angles (°)	(1)	Angles (°)	(2)
S6-Ni1-S9	87.41(4)	S11-Ni1-S12	81.53(2)
S6-Ni1-S16	170.97(5)	S12-Ni1-S21	170.35(2)
S6-Ni1-S19	94.84(4)	S11-Ni2-S12	81.57(2)
S6-Ni1-S6A	83.70(4)	S12-Ni2-S22	89.25(2)
Ni1-S6-Ni1A	96.12(4)	Ni1-S11-Ni2	75.99(2)
Ni1-S6A-Ni1A	96.42(4)	Ni1-S12-Ni2	76.17(2)
S16-Ni1-S19	89.76(4)	S11-Ni1-S21	89.18(2)
S16-Ni1-S6A	89.66(5)	S12-Ni1-S31	97.55(2)
S9-Ni1-S6A	108.47(4)	S11-Ni2-S22	169.37(2)
S19-Ni1-S6A	163.26(5)	S12-Ni2-S32	175.06(2)
S9-Ni1-S16	100.53(4)	S11-Ni1-S31	173.30(2)
S9-Ni1-S19	88.07(4)	S21-Ni1-S31	91.37(2)

Table 4.2: Selected bond lengths (Å) and angles (°) for the complexes **(4)** and **(6)**.

Distances (Å)	(4)	(6)	Distances (Å)	(4)	(6)
Ni1-Se1	2.2929(12)	2.2756(6)	Ni1-S2	2.1932(19)	2.2079(9)
Ni2-Se2	2.2921(12)	2.2788(6)	Ni2-S4	2.1544(18)	2.1444(9)
Ni1-S1	2.1586(19)	2.1396(9)	Ni1-S3	2.1968(18)	2.1855(10)
Ni2-S3	2.2005(18)	2.2161(10)	Ni2-S2	2.1989(18)	2.1810(9)
Angles (°)	(4)	(6)	Angles (°)	(4)	(6)
S2-Ni1-S3	78.49(7)	81.94(3)	S3-Ni1-Se1	94.24(5)	97.30(3)
S3-Ni1-S1	173.44(7)	169.77(4)	S2-Ni2-S4	172.27(7)	170.46(4)
S2-Ni2-S3	78.29(7)	81.94(3)	S3-Ni2-Se2	172.38(7)	175.06(4)
S3-Ni2-S4	98.39(6)	84.16(4)	S2-Ni1-Se1	172.42(7)	176.79(4)
Ni1-S2-Ni2	80.45(5)	75.97(3)	S1-Ni1-Se1	88.69(6)	91.02(3)
Ni1-S3-Ni2	80.33(5)	75.71(3)	S2-Ni2-Se2	94.79(6)	97.30(3)
S2-Ni1-S1	98.76(7)	89.34(3)	S4-Ni2-Se2	88.86(6)	91.28(3)

Table 4.3: Shortest Ni-H_{Me} distances in complexes **(1)**, **(2)**, **(3)**, **(4)** and **(6)**.^a

Distances (Å)	(1)	(2)	(3)	(4)	(6)
Ni-H _{Me}	2.66	3.09	3.26	3.11	3.18
Ni-H _{Me}	2.74	3.16	3.35	3.12	3.11

^a data for **(3)** taken from ref 21.

4.2.3 Reactivity Studies

Compound **(2)** was unexpectedly formed from a solution of **(1)** left for crystallization over two weeks' time. In order to investigate the mechanism of formation of **(2)** from **(1)**, a toluene solution of **(1)** was irradiated using a mercury arc lamp; samples were collected at regular time intervals and were analyzed using ESI-MS spectrometry. Interestingly, the formation of **(2)** is clearly identified from the ESI-MS spectra, showing the gradual disappearance of molecular ion peaks at m/z 326.72 for $[\text{Ni}(\text{ebSmS})+\text{H}]^+$ (**(1)**) with simultaneous growth of the peak corresponding to **(2)** at m/z 238.86 for $[\text{Ni}(\text{emSmS})+\text{H}]^+$ (Fig. AIV.1). When using a mercury lamp the decomposition reaction needs about 12 hours to reach completion with near quantitative formation of **(2)**. In an endeavour to determine the fate of the isobutylenethiolate side arms lost in this reaction, the reaction mixture after irradiation was gently distilled at a temperature of 85 °C. A few drops of a low-boiling product were obtained; ESI-MS spectrometry and NMR spectroscopy (Fig. AIV.2-5) confirmed the identity of (oligo) isobutylene sulfide as the main by-product. The remaining mixture was passed through a neutral alumina column and pure **(2)** was thus obtained in 87% yield. Similarly, the formation of compound **(4)** also occurred from a solution of **(3)** in dichloromethane, left for crystallization over 2-3 weeks' time. To investigate the formation of **(4)** from **(3)** a dichloromethane solution of **(3)** was irradiated using a xenon lamp; samples were collected at regular time intervals and were analyzed using HRMS spectrometry, again showing the gradual disappearance of molecular ion peaks of **(3)** with simultaneous growth of the peak corresponding to **(4)** (Fig. AIV.6). Compound **(3)** needs only two hours of irradiation with the xenon lamp to give complete conversion to compound **(4)**. The formation of compound **(4)** was also monitored with UV-VIS spectroscopy. The dark green compound **(3)** shows a small absorption band at 410 nm with an absorption coefficient ϵ of 480 M⁻¹cm⁻¹. Upon irradiation over 2 h the absorption shifts to 430 nm resulting in a new band with an absorption coefficient of 2300 M⁻¹cm⁻¹ ascribed to the formation of the brown-coloured compound **(4)** (Fig.4.4). The nickel compound of the tetradentate ligand ebSmSe²⁻ could not be isolated; instead

complex **(6)** was formed directly from the reaction mixture. When kept in the dark the compounds **(1)** and **(3)** are found to be rather stable and yield [NiFe] complexes of interest as hydrogenase model systems upon reaction with iron carbonyl complexes (see Chapter 2).^{21,32}

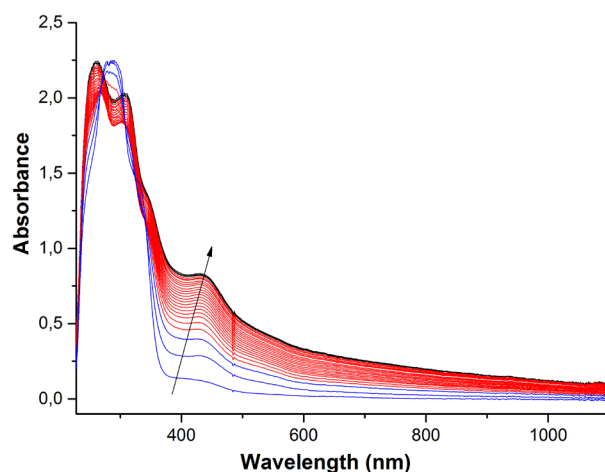


Figure 4.4: Evolution of the UV-VIS spectra of complex **(3)** (1 mM) in dichloromethane upon irradiation with a xenon lamp over 2 h. Spectra were recorded with a transmission dipprobe set at a path length of 2 mm.

4.3 Discussion

In this work we have encountered the unique reactivity of $[\text{Ni}_2(\text{ebSmS})_2]$ **(1)** and $[\text{Ni}(\text{pbSmSe})]$ **(3)** in the formation of the dinuclear low-spin nickel complexes $[\text{Ni}_2(\text{emSmS})_2]$ **(2)** and $[\text{Ni}_2(\text{pmSmSe})_2]$ **(4)** comprising new asymmetric tridentate ligands. However, the nickel complex $[\text{Ni}(\text{ebSmSe})]$ **(5)** could not be isolated and only its decomposition product $[\text{Ni}_2(\text{ebSmSe})_2]$ **(6)** was obtained. The reactivity of the compounds **(1)**, **(3)** and the elusive compound **(5)** is clearly different, which may be related to the difference in ionic radii of the sulfur and selenium donor atoms and the flexibility of the carbon bridge between the two thioether donor atoms in the tetradentate ligands. Both the compounds **(2)** and **(6)** are ‘decomposed’ structures of the ethylene-bridged ligands ebSmS^{2-} comprising thiolate donor atoms and ebSmSe^{2-} having selenolate donor atoms. Whereas the unusual dinuclear structure of compound **(1)** containing 5-coordinate nickel ions indicates that the ethylene-bridged ligand is too strained to accommodate the expected square-planar geometry of the nickel(II) ion, the compound $[\text{Ni}(\text{ebSmSe})]$ **(5)** with the selenolate donor atoms could not be isolated, indicating that the larger radius of the selenolate group induces even more strain in the tetradentate ligand. The propylene bridge in the compounds $[\text{Ni}(\text{pbSmSe})]$ **(3)** and the related thiolate-containing compound $[\text{Ni}(\text{pbSmS})]$ ²⁵ clearly is large enough to accommodate the

square-planar geometry of the nickel ion. However, whereas compound **(3)** with the larger selenolate donor atoms is relatively unstable and decomposes to give **(4)**, the related ‘decomposition’ product so far has not been reported for the thiolate analogue [Ni(pbSmS)].^{25,33}

4.4 Conclusion

In summary, three new nickel(II) complexes were obtained comprising new asymmetric tridentate thioether-dithiolate or thioether-thiolate-selenolate ligands. The nickel thiolate compound **(1)** presented here shows a novel coplanar dinuclear structure with 5-coordinate nickel centers involved in Ni...H anagostic interactions. Upon irradiation of this compound clean conversion to the ‘decomposed’ compound **(2)** with the concomitant release of oligo-isobutylene sulfide is observed, which must occur through light-induced C–S and Ni–S bond cleavage. The broad signals observed in ¹H NMR spectra of **(1)**, the short Ni–S distances observed in the X-ray crystal structure in combination with the unusual disorder are indicative of the presence of partial Ni(I)-S’ character. Further exploration of this light-induced reaction with a combination of spectroscopic techniques and the study of the reactivity of **(1)** and **(3)** with other substrates or small molecules are in progress and may shed light onto the reaction pathway and pave the way toward new organosulfur derivatives.

4.5 Experimental

4.5.1 Materials

All experiments were performed using standard Schlenk techniques or in a glovebox under an argon or nitrogen atmosphere unless otherwise noted. Chemicals were purchased from Acros or Aldrich and were used without further purification. Organic solvents were deoxygenated by the freeze-pump-thaw method and were dried over molecular sieves prior to use. The NMR solvent CD₂Cl₂ for the metal complexes was deoxygenated by the freeze-pump-thaw method and was stored over molecular sieves in a glovebox. Complex **(3)** was synthesized according to a published procedure.²¹

4.5.2 Physical Measurements

NMR spectra were recorded on a 300 MHz Bruker DPX 300 spectrometer and chemical shifts were referenced against the solvent peaks. Mass spectra were obtained with a Finnigan TSQ quantum instrument using ESI. HRMS was recorded on a Thermo Scientific LTQ Orbitrap XL high resolution FT-MS system. Elemental analyses were performed by the

Microanalytical Laboratory Kolbe in Germany. Irradiations were carried out at room temperature using a Hanau TQ81 high-pressure mercury arc lamp for complex **(1)** and a Lot Xenon lamp for complex **(3)** with continuous stirring. UV-vis spectra were collected using a transmission dipprobe with 2 mm path length on an Avantes Avaspec-2048 spectrometer with Avalight-DH-S-BAL light source.

4.5.3 Single Crystal X-ray Crystallography

X-ray intensities for **(1)** and **(2)** were measured on a Nonius KappaCCD diffractometer with rotating anode (graphite monochromator, $\lambda = 0.71073 \text{ \AA}$). Intensity integration was performed with EvalCCD³⁴ (for **(1)**) or HKL2000³⁵ (for **(2)**). Absorption correction was based on multiple measured reflections. The structures were solved with SHELXS-97³⁶ using Direct Methods and refined against F^2 of all reflections using SHELXL-2016/6.³⁷ Non-hydrogen atoms were refined freely with anisotropic displacement parameters. Hydrogen atoms were introduced in calculated positions and refined with a riding model. Geometry calculations and checking for higher symmetry was performed with the PLATON program.³⁸ The reflection intensities for **(4)** and **(6)** were measured at 110(2) K using a SuperNova diffractometer (equipped with Atlas detector) with Cu $K\alpha$ radiation ($\lambda = 1.54178 \text{ \AA}$) under the program CrysAlisPro (Version 1.171.36.32 Agilent Technologies, 2013). The same program was used to refine the cell dimensions and for data reduction. The structure was solved with the program SHELXS-2014/7 and was refined on F^2 with SHELXL-2014/7.³⁷ Analytical numeric absorption correction using a multifaceted crystal model was applied using CrysAlisPro. The temperature of the data collection was controlled using the system Cryojet (manufactured by Oxford Instruments). The H atoms were placed at calculated positions (unless otherwise specified) using the instructions AFIX 23 or AFIX 137 with isotropic displacement parameters having values 1.2 or 1.5 U_{eq} of the attached C atoms. Both structures are ordered.

4.5.4 Synthesis of 4,7-dithia-2,9-dimethyldecane-2,9-diol: To a solution of 1,2-ethanedithiol (5.65 g, 60 mmol) in 70 ml ethanol was added 1-chloro-2-methyl-2-propanol (13.03 g, 120 mmol) and NaOH (4.81 g, 120 mmol) in 45 ml water. After refluxing for two hours, the formed NaCl was removed by filtration. After evaporating the ethanol under reduced pressure, water was added and the product was extracted with chloroform. The combined chloroform layers were dried with $MgSO_4$ and evaporated to get 10.68 g of a colorless oil (98%). 1H NMR: δ_H [300.13 MHz, $CDCl_3$, 298 K] 2.78 (m, 2H, $-OH$), 2.70 (s, 4H, $-S-CH_2-C(CH_3)_2OH$), 2.57 (s, 4H, $-S-CH_2-CH_2-S-$) 1.62 (s, 12H, $-C(CH_3)_2OH$). ^{13}C

NMR: δ_C [75.47 MHz, $CDCl_3$, 298 K] 70.3 ($-C(CH_3)_2OH$), 46.4 ($-S-CH_2-C(CH_3)_2OH$), 34.1 ($-S-CH_2-CH_2-S-$), 28.3 ($-(CH_3)_2OH$).

4.5.5 Synthesis of 1,8-dichloro-3,6-dithia-2,2,7,7-tetramethyloctane: To a solution of 4,7-dithia-2,9-dimethyldecane-2,9-diol (10.68 g, 58.72 mmol) in 20 ml $CHCl_3$ was added dropwise a solution of $SOCl_2$ (17.85 g, 150 mmol) in $CHCl_3$. The color of the solution initially turned in yellow and orange at the final stage of the addition of $SOCl_2$. After an hour stirring the chloroform and excess $SOCl_2$ were evaporated under reduced pressure to yield 12.33 g of a yellow oil (quantitative yield). 1H NMR: δ_H [300.13 MHz, $CDCl_3$, 298 K] 2.93 (s, 4H, $-CH_2-Cl$), 2.81 (s, 4H, $-S-CH_2-CH_2-S-$), 1.62 (s, 12H, $-CH_3$). ^{13}C NMR: δ_C [75.47 MHz, $CDCl_3$, 298 K] 70.0 ($-CH_2-Cl$), 48.01 ($-S-CH_2-CH_2-C(CH_3)_2Cl$), 34.3 ($-S-CH_2-CH_2-S-$), 31.3 ($-CH_3$).

4.5.6 Synthesis of 1,8-dithiuronium-3,6-dithia-2,2,7,7-tetramethyloctane dichloride: Thiourea (7.99 g, 105 mmol) and 1,8-dichloro-3,6-dithia-2,2,7,7-tetramethyloctane (12.11 g, 55.24 mmol) were dissolved in ethanol (85 ml) and refluxed for one hour. After 30 min an off-white precipitate was formed. The solution was allowed to cool, the solid product was collected by filtration, washed with cold ethanol and diethyl ether, and dried under vacuum to get 17.64 g of the pure compound (76%). 1H NMR: δ_H [300.13 MHz, $DMSO-d_6$, 298 K] 9.33 (d, 8H, $-SC^+(NH_2)_2Cl^-$) 3.56 (s, 4H, $-CH_2-SC^+(NH_2)_2Cl^-$), 2.71 (s, 4H, $-S-CH_2-CH_2-S-$), 1.31 (s, 12H, $-CH_3$). ^{13}C NMR: δ_C [75.47 MHz, $DMSO-d_6$, 298 K] 170.3 ($-CH_2-SC^+(NH_2)_2Cl^-$), 45.5 ($-CH_2-SC^+(NH_2)_2Cl^-$), 42.5 ($-S-C(CH_3)_2-$) 28.0 ($-S-CH_2-CH_2-S-$), 27.5 ($-CH_3$). MS (ESI): (m/z) calculated for $C_{12}H_{27}S_4N_4 [M-2Cl-H]^+$ requires (monoisotopic mass) 355.11, found 354.74.

4.5.7 Synthesis of 1,8-diselenouronium-3,6-dithia-2,2,7,7-tetramethyloctane dichloride: A solution of selenourea (594 mg, 4.83 mmol) in 5 ml ethanol was added to a solution of 1,8-dichloro-3,6-dithia-2,2,7,7-tetramethyloctane (665 mg, 2.42 mmol) in 5 ml ethanol; the reaction mixture was refluxed for 30 min. The solution was allowed to cool, and the solid product was collected by filtration. The product was washed with cold ethanol and diethyl ether, and dried in vacuo yielding 1.07 g of pure compound (85%). 1H NMR: δ_H [300.13 MHz, $DMSO-d_6$, 298 K] 9.39 (d, 8H, $-SeC^+(NH_2)_2Cl^-$) 3.62 (s, 4H, $-CH_2-SeC^+(NH_2)_2Cl^-$), 2.77 (s, 4H, $-S-CH_2-CH_2-S-$), 1.37 (s, 12H, $-CH_3$). ^{13}C NMR: δ_C [75.47 MHz, $DMSO-d_6$, 298 K] 166.92 ($-CH_2-SeC^+(NH_2)_2Cl^-$), 45.69 ($-CH_2-SeC^+(NH_2)_2Cl^-$), 40.55 ($-S-C(CH_3)_2-$) 28.13

(–S–CH₂–CH₂–S–), 28 (–CH₃). MS (ESI): (*m/z*) calculated for [M–2Cl]²⁺ requires (monoisotopic mass) 225.21, found 224.4.

4.5.8 Synthesis of [Ni₂(ebSmS)₂] (1): To a two-necked flask charged with a solution of Ni(acac)₂ (0.768g, 3 mmol) in 60 ml dry toluene was added the ligand as the dithiuronium dichloride precursor of the ligand H₂ebSmS (1.284 g, 3 mmol). After 10 minutes stirring at 50 °C, NMe₄OH (2.73 ml, 6 mmol) was added to the mint-green solution, resulting in a colour change to dark brown. The reaction mixture was refluxed for three hours. After evaporating the solvent, CH₂Cl₂ was added and the insoluble by-products were removed by filtration. The filtrate was passed through alumina and the first dark-red band was collected and evaporated to yield 0.14 g of pure [Ni₂(ebSmS)₂] (**1**) (15%). Performing the reaction and the following work-up procedure in darkness drastically improved the yield to 63%. Elemental Analysis (%): Calculated for C₂₀H₄₀S₈Ni₂·0.4CH₂Cl₂: C 35.59, H 5.97, S 37.26; found C 35.57, H 5.98, S 37.19. MS (ESI): (*m/z*) calculated for C₁₀H₂₁S₄Ni [M/2+H]⁺ requires (monoisotopic mass) 326.99, found 326.72.

4.5.9 Formation of [Ni₂(emSmS)₂] (2): Compound (**1**) (0.98 g, 3 mmol) was dissolved in 50 ml toluene and the solution was irradiated using a Hanau TQ81 high-pressure mercury arc lamp. Completion of the reaction was monitored by recording ESI-MS spectra of the samples collected in regular intervals. The reaction needed 12 hrs for completion; the formed isobutylene sulfide was collected from the reaction mixture by gentle distillation. Oligo-isobutylene sulfide started to distill over when the temperature was around 85 °C; the collection flask was kept at 0 °C using an ice bath. The remaining mixture was passed through a neutral alumina column and pure (**2**) was thus obtained in 87% yield. Elemental Analysis (%): Calculated for C₁₂H₂₄S₆Ni₂: C 30.15, H 5.06, S 40.24; found C 30.27, H 5.18, S 40.29. MS (ESI): (*m/z*) calculated for C₆H₁₃S₃Ni [M/2+H]⁺ requires (monoisotopic mass) 238.95, found 238.86.

4.5.10 Formation of [Ni₂(pmSmSe)₂] (4): Compound (**3**) was dissolved in dichloromethane and the solution was irradiated using a LOT xenon lamp. Completion of the reaction was monitored by recording HRMS spectra of the samples collected in regular intervals. The reaction needed 2 hrs of irradiation to reach completion. Crystals of (**4**) were obtained by vapor diffusion of pentane into the DCM solution of (**3**) in daylight. HR-MS (CH₂Cl₂): (*m/z*) calculated for C₁₄H₂₈Ni₂S₄Se₂ [M+H]⁺ requires (monoisotopic mass) 599.8095, found

599.8111. Elemental Analysis (%): Calculated for C₁₄H₂₈Ni₂S₄Se₂: C 28.03, H 4.70; found C 28.08, H 4.71.

4.5.11 [Ni(ebSmSe)] (5): A solution of NMe₄OH (164 mg, 0.906 mmol) and ligand precursor (1,8-diselenouronium-3,6-dithia-2,2,7,7-tetramethyloctane dichloride) (236 mg, 0.453 mmol) were dissolved in 30 ml ethanol and mixed with Ni(acac)₂ (116 mg, 0.453 mmol) in 30 ml toluene. This immediately resulted in a colour change to dark reddish-brown. Unfortunately, a pure compound could not be isolated.

4.5.12 [Ni₂(emSmSe)₂] (6): A solution of NMe₄OH (164 mg, 0.906 mmol), the dithiouronium dichloride precursor of the ligand H₂ebSmSe (236 mg, 0.453 mmol) and Ni(acac)₂ (116 mg, 0.453 mmol) were refluxed in 60 ml ethanol for 1 h. The solvent was evaporated until approximately 10 ml solvent remained, resulting in a brown precipitate. The solid was collected by filtration and washed with ethanol. Yield: 133.7 mg (52%) MS (ESI): (*m/z*) calculated for C₁₂H₂₄S₄Se₂Ni₂ [M+H]⁺ requires 572.79, (monoisotopic mass) found 572.78. Elemental Analysis (%): Calculated for C₁₂H₂₈Ni₂S₄Se₂: C 25.20, H 4.23; found C 25.26, H 4.21.

4.6 Acknowledgements

G. K. Spijksma is gratefully acknowledged for HRMS measurement and J.J.M. van Brussel is gratefully acknowledged for ESI-MS measurements.

4.7 References

1. C. Tard and C. J. Pickett, *Chem. Rev.*, 2009, **109**, 2245.
2. V. Mathrubootham, J. Thomas, R. Staples, J. McCracken, J. Shearer and E. L. Hegg, *Inorg. Chem.*, 2010, **49**, 5393.
3. J. Shearer, K. P. Neupane and P. E. Callan, *Inorg. Chem.*, 2009, **48**, 10560.
4. R. Angamuthu, L. L. Gelauff, M. A. Siegler, A. L. Spek and E. Bouwman, *Chem. Commun.*, 2009, 2700.
5. K. N. Green, S. M. Brothers, B. Lee, M. Y. Darensbourg and D. A. Rockcliffe, *Inorg. Chem.*, 2009, **48**, 2780.
6. U. Ermler, *Dalton Trans.*, 2005, 3451.
7. U. Ermler, W. Grabarse, S. Shima, M. Goubeaud and R. K. Thauer, *Science*, 1997, **278**, 1457.
8. T. Wongnate and S. W. Ragsdale, *J. Biol. Chem.*, 2015, **290**, 932.
9. S. Castellano, A. V. Lobanov, C. Chapple, S. V. Novoselov, M. Albrecht, D. Hua, A. Lescure, T. Lengauer, A. Krol, V. N. Gladyshev and R. Guigo, *Proc. Natl. Acad. Sci. USA.*, 2005, **102**, 16188.
10. J. A. Gámez, M. Yáñez, *Chem. Commun.*, 2011, **47**, 3939.

11. V. Pelmeshnikov and P. E. M. Siegbahn, *J. Biol. Inorg. Chem.*, 2003, **8**, 653.
12. V. Pelmeshnikov, M. R. A. Blomberg, P. E. M. Siegbahn and R. H. Crabtree, *J. Am. Chem. Soc.*, 2002, **124**, 4039.
13. E. C. Duin and M. L. McKee, *J. Phys. Chem. B*, 2008, **112**, 2466.
14. T. Wongnate, D. Sliwa, B. Ginovska, D. Smith, M. W. Wolf, N. Lehnert, S. Raagei and S. W. Ragsdale, *Science*, 2016, **352**, 6288.
15. A. Beganskiene, L. R. Pignotti, V. Baltramiejunaite, R. L. Luck and E. Urnezis, *Inorg. Chim. Acta*, 2008, **361**, 1349.
16. M. D. Curtis and S. H. Druker, *J. Am. Chem. Soc.*, 1997, **119**, 1027.
17. J. S. Kim, J. H. Reibenspies and M. Y. Darensbourg, *J. Am. Chem. Soc.*, 1996, **118**, 4115.
18. J. S. Kim, J. H. Reibenspies and M. Y. Darensbourg, *Inorg. Chim. Acta*, 1996, **250**, 283.
19. M. Y. Cha, S. C. Shoner and J. A. Kovacs, *Inorg. Chem.*, 1993, **32**, 1860.
20. D. Sellmann and W. Reisser, *J. Organomet. Chem.*, 1985, **294**, 333.
21. G. Gezer, D. Duran Jiménez, M. A. Siegler and E. Bouwman, *Dalton Trans.*, 2017, **46**, 7506.
22. J. A. W. Verhagen, M. Lutz, A. L. Spek and E. Bouwman, *Eur. J. Inorg. Chem.*, 2003, 3968.
23. J. A. W. Verhagen, D. D. Ellis, M. Lutz, A. L. Spek and E. Bouwman, *Dalton Trans.*, 2002, 1275.
24. R. Angamuthu, H. Kooijman, M. Lutz, A. L. Spek and E. Bouwman, *Dalton Trans.*, 2007, 4641.
25. K. Weber, I. Heise, T. Weyhermüller and W. Lubitz, *Eur. J. Inorg. Chem.* 2014, 148.
26. D. Sellmann, D. Haussinger and F. W. Heinemann, *Eur. J. Inorg. Chem.*, 1999, 1715.
27. R. Cao, M. C. Hong, F. L. Jiang, X. L. Xie and H. Q. Liu, *Dalton Trans.*, 1994, 3459.
28. C. Wombwell and E. Reisner, *Chem. Eur. J.* 2015, **21**, 8096.
29. C. Zhang, S. Takada, M. Kölzer, T. Matsumoto and K. Tatsumi, *Angew. Chem.-Int. Edit.*, 2006, **45**, 3768.
30. M. Brookhart, M. L. H. Green and G. Parkin, *Proc. Natl. Acad. Sci. U. S. A.*, 2007, **104**, 6908.
31. M. K. Yadav, G. Rajput, L. B. Prasad, M. G. B. Drew and N. Singh, *New J. Chem.*, 2015, **39**, 5493.
32. R. Angamuthu, PhD Thesis, *Structural and Functional Models for [NiFe] Hydrogenase*, Leiden University, Leiden, 2009.
33. K. Weber, O. F. Erdem, E. Bill, T. Weyhermüller and W. Lubitz, *Inorg. Chem.*, 2014, **53**, 6329.
34. A. J. M. Duisenberg, L. M. J. Kroon-Batenburg, A. M. M. Schreurs, *J. Appl. Cryst.*, 2003, **36**, 220.
35. Z. Otwinowski, W. Minor, *Methods in Enzymology*, (C.W. Carter, Jr. & R.M. Sweet, Eds) Academic Press, 1997, **276**, 307.
36. G. M. Sheldrick, *Acta Cryst.*, 2008, **A64**, 112.
37. G. M. Sheldrick, *Acta Cryst.*, 2015, **C71**, 3.
38. A. L. Spek, *J. Appl. Cryst.*, 2003, **36**, 7.